Detection of the Oxidation Area by Spectrophotometry: Regional and Temporal Changes in Anodic Oxidation on Titanium in Bipolar Electrochemistry

Yuuka Kokubo and Hidetaka Asoh*

ACCESS | Metrics & More | Article Recommendations | Supporting Information

ABSTRACT: This study investigated the temporal change in the oxidation area on a titanium (Ti) bipolar electrode (BPE) subjected to bipolar anodization in a direct current (DC) electric field using a spectrophotometer. The rectangular Ti sheet used as a BPE was horizontally positioned at the center of a cell. After the DC bipolar anodization, the oxidized area was detected nondestructively and visually using a specific interference color that depends on the thickness of the barrier-type oxide film formed on the Ti BPE. The change in the $L*a*b*$ color space corresponding to each interference color revealed that the oxidation area increased along the longitudinal axis of the BPE with the increasing electrolysis time by reflecting the change in the potential distributions on the BPE. As visually demonstrated, the area where the anodic reaction proceeded reached saturation at 90% of the BPE surface area.

Temporal change in the oxidation area
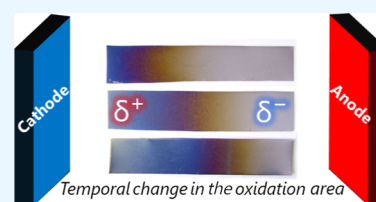
INTRODUCTION

Bipolar electrochemistry attracts attention as a powerful tool for designing asymmetric functional surfaces and a straightforward synthetic route to Janus particles with anisotropic chemical composition and structure.[1−8] Most studies on bipolar electrochemistry adopted an open bipolar cell under a direct current (DC) electric field. In these works, a plate-like bipolar electrode (BPE) horizontally positioned at the center of two driving electrodes in the cell is generally used. Although the BPE does not require a direct electrical connection to the external power supply, reduction−oxidation (redox) reactions simultaneously occur in pairs at the opposite ends of the BPE under a potential gradient in a DC electric field. The maximum potential difference over the plate-like BPE (ΔV_{BPE}) can be estimated as follows using eq 1.[1,2]

$$\Delta V_{BPE} = E \ (l/L) \tag{1}$$

ΔV_{BPE} is generally considered to be governed by the voltage applied to the driving electrodes (E), the distance between the driving electrodes (L), and the BPE length (l).[1,2] However, this equation does not consider the changes over time and the influence of the environment around the BPE (e.g., type, volume, and conductivity of the electrolyte). In terms of the electroneutrality principle, it is also sometimes misunderstood that the area balance of the anode and the cathode on the BPE is the same, and the area is divided into two regions at the center of the horizontally positioned BPE. For example, the redox area of bipolar anodization is not evenly divided.[3,4,6,9,10] Nevertheless, only a few detailed studies on the temporal changes in the reaction area were made.

In our previous studies, we adopted bipolar electrochemistry as the surface treatment of light metals (i.e., bipolar anodization)

and investigated the effects of electrolytic conditions (e.g., concentration and temperature of the electrolyte, type of electric field, and electrode configuration) on the structures of the formed oxide films.[11−18] When aluminum BPE was horizontally positioned at the center of a cell, the area of the anodic reaction (anodic film formation) was much larger than expected, accounting for 90% of the BPE.[15] Although bipolar anodization has a potential for prospective surface treatments due to its design flexibility based on a wireless operation, the change in the area of the region, in which the redox reactions proceed, has not yet been completely clarified.

This study systematically investigates the regional and temporal changes in anodic oxidation on a BPE under a DC electric field using a spectrophotometer. As previously reported,[17] titanium (Ti) was used as a BPE to visually and simply evaluate the temporal change in the reaction area. The surface of the anodized Ti exhibited specific interference colors due to the high dielectric constant of the oxide films that formed it;[19−21] hence, the anodic reaction area can be nondestructively and visually identified using the spectrophotometry technique. Moreover, the effective voltage that directly contributed to the film formation was estimated along the longitudinal axis of the BPE by evaluating the $L*a*b*$ color space corresponding to each interference color, which depended on the thickness of the barrier-type oxide film formed on the Ti BPE.

EXPERIMENTAL SECTION

Two driving electrodes [carbon plates, 12 cm (H) × 4.2 cm (W) × 0.8 cm (D)] were positioned 7 cm apart at both ends of a plastic container. A Ti sheet (99.5%, Nilaco Corporation) cut into a rectangular shape (1 cm × 5 cm) was degreased with acetone for 3 min, chemically polished in an HF (46%)-HNO$_3$ (60%) mixture (1:4) for 3 min in an ice bath, and then rinsed with deionized water. The Ti BPE was horizontally positioned at the center of the cell (Figure 1). One side (upside surface) of each Ti BPE was exposed to the electrolyte by covering the back (downside surface) with Kapton tape.
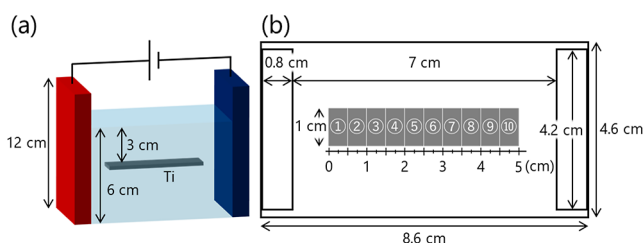

Figure 1. (a) Schematic of the bipolar anodization. (b) Top view of the cell used for the bipolar anodization.

DC bipolar anodization was performed in 200 mL of 0.01 mol dm^{-3} phosphoric acid at 20 °C by applying 60 V of DC voltage between the driving electrodes for various times. It is well known that compact oxide films can be formed with fluoride-free electrolytes (e.g., sulfuric acid, acetic acid, phosphoric acid, and sodium hydroxide).[19] Here, phosphoric acid was selected as the electrolyte because it is easier to handle than other electrolytes. The electrolyte was stirred at 300 rpm with a magnetic stirrer during bipolar anodization to maintain a constant temperature of 20 °C.

The UV−vis reflectance spectra were measured using a spectrophotometer to evaluate the thickness distribution of the formed film on the BPE after electrolysis (KONICA MINOLTA, CM-5). The measurements were performed at the center of each section, which was divided into 10 sections of 0.5 × 1 cm^2 section (①−⑩ in Figure 1b). A target mask with a 5 mm-diameter aperture was used to focus on the measurement area for the reflectance measurement. The interference colors were evaluated using the reflectance spectra of the CIE1976 L*a*b* color space standardized by the Commission Internationale de l'Eclairage. The CIE L*a*b* color space was determined according to DIN 5033, 2° observer, illuminant D$_{65}$, as described in our previous study.[12] The morphology of the film developed on Ti was evaluated using field-emission scanning electron microscopy (FESEM, JEOL JSM-6701F), while its crystallographic structure was evaluated using X-ray diffractometry (XRD, Rigaku SmartLab).

The change in the L*a*b* color space of the bipolar anodization system was compared with that of the conventional anodization system to estimate the effective voltage that contributed to the film formation on the BPE. Therefore, the relationship between the interference color and the formation voltage of conventional anodization was also investigated for reference. The conventional anodization of Ti was conducted in 0.01 mol dm^{-3} phosphoric acid at 20 °C with voltages ranging from 5 to 50 V.

RESULTS AND DISCUSSION

Conventional Anodization of Ti. Anodized Ti specimens were prepared by conventional anodization from 5 to 50 V to investigate the relationship between the interference color and
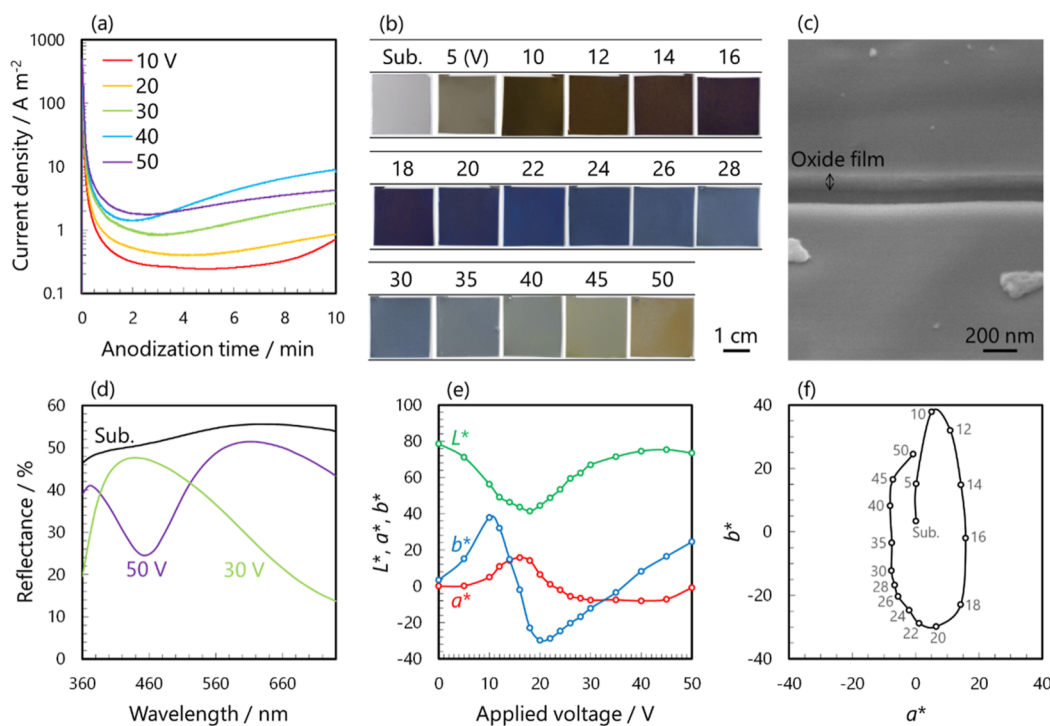

Figure 2. (a) Current density−time curves for the Ti sheet anodization at a constant voltage. (b) Digital photographs of the Ti sheets after anodization at different applied voltages. (c) Cross-sectional SEM image of the Ti sheet after anodization at 50 V. (d) UV−vis reflectance spectra. (e) Relationship between the L*a*b* values and the applied voltage. (f) a*b* color space of the Ti specimens after anodization at different applied voltages.

the formation voltage. Figure 2a shows the typical current density−time curves for the Ti sheet anodization at a constant voltage. For all cases, the current density increased at the initial stage of anodization and then decreased to a range from 10 to 0.1 A m^{-2}, indicating the formation of a barrier-type oxide film. Figure 2b depicts the surface appearances of the anodized Ti sheets. The oxide film formed on the Ti sheets became thicker as the applied voltage increased, and the interference color changed from gold, pink, blue, and light blue to yellow as the oxide film thickness increased. This color change was similar to that of the oxide films formed on Ti in the previous studies.[19−21] The actual thickness of the film formed on Ti can be roughly estimated using the voltage−thickness relationship reported by Van Gils et al.[20] Figure 2c shows a cross-sectional SEM image of the Ti sheet after anodization at 50 V. A uniform compact oxide film with a thickness of ∼100 nm was formed on Ti. The surface was flat without nanopores. XRD characterization was performed to understand the structure of the Ti oxide film (Figure S1 in the Supporting Information). Although the XRD spectra exhibited many diffraction peaks, the pattern corresponded to metallic Ti. Diffraction peaks of crystalline Ti oxide (e.g., anatase and rutile) cannot be observed on the diffraction pattern in Figure S1; hence, the formed film is considered amorphous Ti oxide.

Figure 2d shows the UV−vis reflectance spectra for the Ti sheets anodized at 30 and 50 V. The number of oscillations with peaks and valleys for the Ti anodized at 50 V was larger than that of the specimen anodized at 30 V. The film thickness increased with the applied voltage increase. Figure 2e shows the relationship between the $L*a*b*$ values and applied voltages. Table S1 in the Supporting Information shows the $L*a*b*$ values obtained using the reflectance spectra. Here, $L*$ indicates lightness. The color changes were analyzed in detail by performing a color evaluation not only on the samples shown in Figure 2a but also on the anodized Ti sheets prepared by varying the applied voltage in 2 V increments from 10 to 20 V. Each value continuously varied from the substrate (0 V) to the specimen anodized at 50 V. Figure 2f illustrates the $a*b*$ color space measured by a spectrophotometer. The $a*$ and $b*$ axes represent the red/green and yellow/blue components, respectively. For the $a*$ axis, positive values indicate red, whereas negative values indicate green. While for the $b*$ axis, positive values indicate yellow, whereas negative values indicate blue. The $a*b*$ values of the anodized samples changed circle clockwise around the substrate value ($a* = 0.07$ and $b* = 3.41$) as the applied voltage increased. This voltage dependence of the color change was used to estimate the effective voltage on the BPE, which will be described below.

Current−Time Curve for the DC Bipolar Anodization of Ti. Figure 3 shows the typical current−time curves for the DC bipolar anodization. The current density was calculated for the apparent surface area (24 cm^2) of one carbon electrode. Although two paths were available for the ion and electron currents flowing through the electrolyte and the BPE in the cell, the exposed Ti surface area can be ignored for the current density calculation because the current was measured at a circuit between two driving electrodes. The current density at the steady state was approximately 170 A m^{-2}, regardless of the electrolysis time. This indicated the good reproducibility of the DC bipolar anodization of Ti.

Figure 4 presents the surface appearances of the Ti BPEs after the DC bipolar anodization for 2, 5, 10, and 30 s and 1, 2, and 10 min. The Ti sheets were horizontally positioned to visually
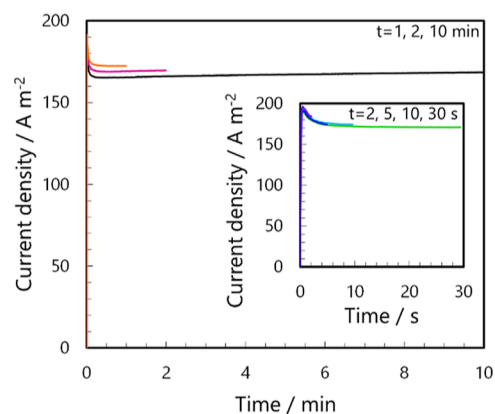

Figure 3. Current density−time curves for the DC bipolar anodization of Ti in 0.01 mol dm^{-3} phosphoric acids at 20 °C at 60 V.
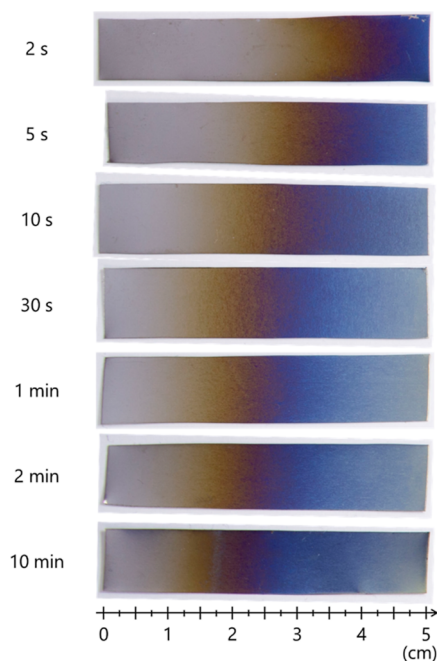

Figure 4. Digital photographs of the Ti sheets after the DC bipolar anodization for different durations.

investigate the temporal change in the reaction area on the BPEs (Figure 1). Interference fringes were observed along the longitudinal axis of each specimen. Although this study focused only on the upside surface, similar interference fringes were observed on both surfaces when the downside surface was exposed without a masking process (Figure S2).

The thickest film was formed at position ⑩ in an anodic area of the BPE facing the driving electrode used as a cathode. The film thickness gradually decreased in the direction of the cathodic area of the BPE facing the driving electrode used as an anode. The leftmost region ① exhibited a metallic luster, implying no film formation. Therefore, the left edge of the BPE was considered to act as a local cathode on the BPE. These findings are generally consistent with those of the previous results on the bipolar Ti anodization.[3,4]

Estimation of the Effective Voltage Contributed to the Film Formation on the Ti BPE. The UV−vis reflectance spectra were measured at the center of each section (①−⑩) to evaluate the thickness of the barrier-type oxide films formed on the BPE. Tables S2−S7 in the Supporting Information list the
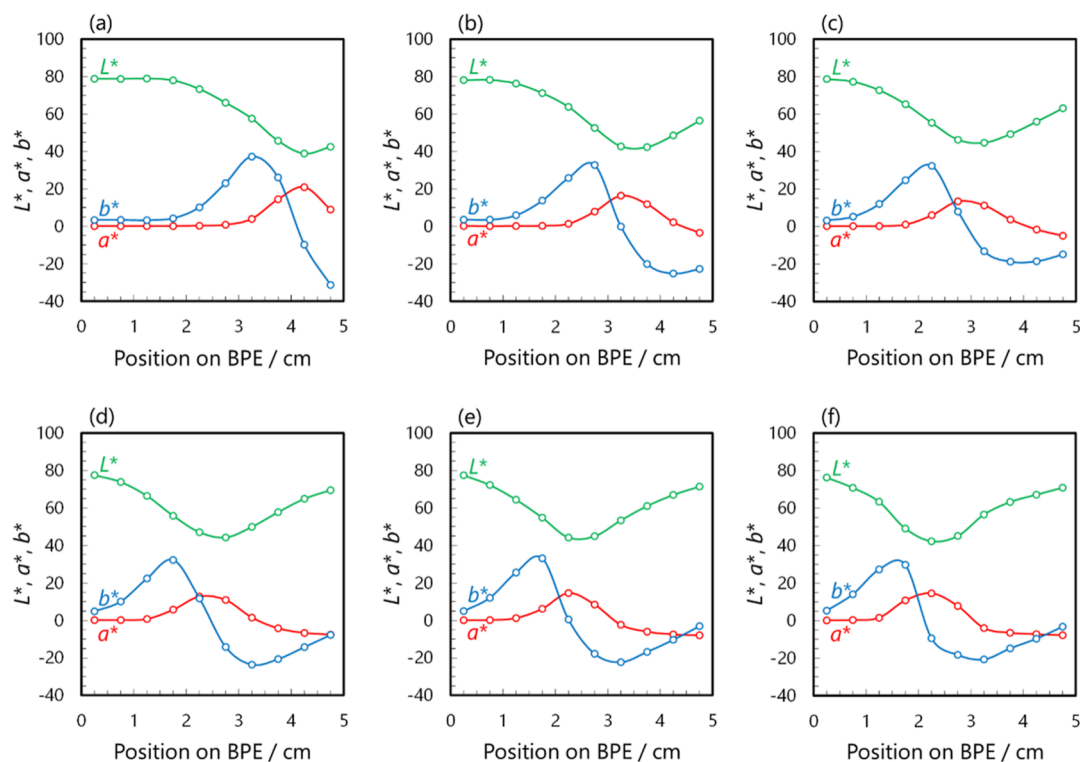
Figure 5. Relationship between the $L^*a^*b^*$ values and their corresponding measured positions of the Ti specimens after the DC bipolar anodization for (a) 2, (b) 5, (c) 10, and (d) 30 s and (e) 1 and (f) 2 min.

$L^*a^*b^*$ values of the samples after DC bipolar anodization for 2, 5, 10, and 30 s and 1 and 2 min. Figure 5 shows the relationship between the $L^*a^*b^*$ values and their corresponding measured positions. Figure S3 shows the a^*b^* color space corresponding to each interference color.

Here, the color changes in the sample after the DC bipolar anodization for 10 min were analyzed in detail. Table 1 lists the

Table 1. $L^*a^*b^*$ Values and Actual Colors of the Ti Specimens after the DC Bipolar Anodization for 10 min

position on BPE/cm	L^*	a^*	b^*	color
①	0.25	77.72	0.07	4.88	gray
②	0.75	75.07	0.12	9.09	gray−gold
③	1.25	63.96	1.30	27.70	gold
④	1.75	51.81	7.57	30.14	gold−pink
⑤	2.25	42.54	15.73	−3.07	purple
⑥	2.75	46.45	5.14	−24.34	purple−dark blue
⑦	3.25	55.45	−3.36	−20.69	dark blue
⑧	3.75	64.78	−6.68	−13.16	blue
⑨	4.25	71.16	−7.70	−4.16	light blue
⑩	4.75	73.96	−8.25	2.55	light blue−yellow

$L^*a^*b^*$ values obtained from the spectrophotometric measurements and their corresponding actual colors. The $L^*a^*b^*$ values were plotted against the position on the BPE (Figure 6a). The values continuously varied from ① to ⑩ along the longitudinal axis of the BPE. Figure 6b shows the a^*b^* color space corresponding to each interference color. The a^*b^* values changed circle clockwise around the ① value ($a^* = -8.25$ and $b^* = 2.55$). The results in Figure 6a,b display the same trend as for the constant voltage anodization in Figure 2e,f, indicating the voltage dependence of the color change. The results in Figures 5
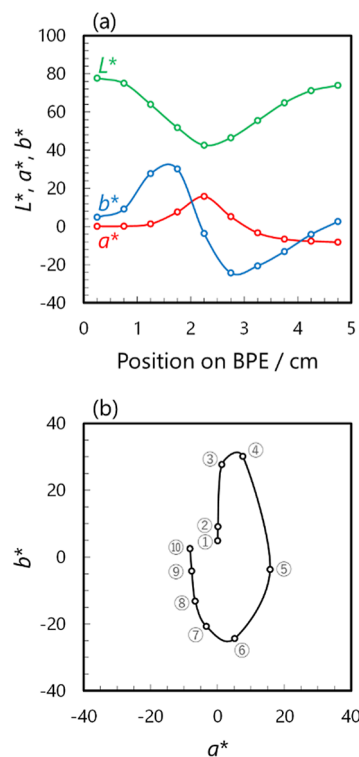

Figure 6. (a) Relationship between the $L^*a^*b^*$ values and their corresponding measured positions and (b) the a^*b^* color space of the Ti specimens after the DC bipolar anodization for 10 min.

and S3 also display similar trends. From the relationship between the film thickness and the corresponding interference color,[19] the thickness of the film formed on the Ti BPE after the DC bipolar anodization for 10 min was roughly estimated to

vary in the 0 to 70 nm range. While the leftmost region ①
exhibited a metallic luster, implying the absence of film
formation, the thickness at the center of the rightmost region
⑩ was estimated to be ∼60 nm using the corresponding color.

Figure 7 illustrates the relationship between the effective
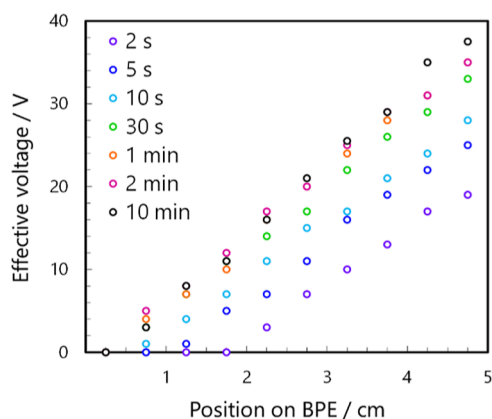voltage and the corresponding measured position. The effective

Figure 7. Relationship between the estimated effective voltage and the
corresponding measured position on the BPE for the DC bipolar
anodization.

voltages were estimated by applying the voltage dependence of
the color change in Figure 2 as a calibration curve. The higher
the effective voltage, the thicker the barrier-type oxide film
formed. This variation in the estimated effective voltage
indicated that the effective voltage was graduated. The effective
voltage almost linearly increased from the left side ① of the Ti
BPE to the opposite side ⑩. In Figure 7, the zero potential area
was considered as ∼2 cm from the left edge of the BPE for 2 s.
For 5 and 10 s, the zero potential area decreased to ∼1 and 0.5
cm from the left edge. In other words, the area of the anodic
reaction on the BPE increased to 60% at 2 s and 80% at 5 s and
saturated at 90% over 10 s.

At the initial stage of the DC bipolar anodization, the oxidized
area was approximately half of the BPE surface, but the area of
the anodic reaction on the BPE expanded over time, as described
above. Wei et al. reported that a TiO$_2$ nanotube-size gradient
covers a large part (approximately 75%) of the Ti BPE during
the DC bipolar anodization.[4] Mu et al. also reported that the
TiO$_2$ nanotube gradient took up more than 80% of the BPE

surface after the bipolar anodization.[6] In their case, an electrolyte
containing a fluoride ion was used to form a TiO$_2$ nanotube with
different dimensions. In contrast, the electrolyte used herein was
phosphoric acid without fluoride ions, which resulted in the
formation of a barrier-type compact film. The electrical
insulating properties of the barrier-type TiO$_2$ film formed in
phosphoric acid were higher than those of the barrier layer of the
porous TiO$_2$ film formed in the electrolyte containing a fluoride
ion. Therefore, the area of the anodic reaction expanded beyond
75% of the BPE area and reached saturation at 90%. In
conclusion, the oxidized area should become much larger than
the area acting as a local cathode due to the temporal change in
the passivation region on the Ti BPE.

The temporal color change in each section of the BPE was
then investigated. Figure 8a shows a typical a*b* color space
corresponding to the ⑤ and ⑩ positions. In the case of position
⑤, the a*b* values changed in a clockwise half circle around the
2 s value (a* = 9.00 and b* = −31.27) as the reaction time
increased from 2 s to 10 min. In the case of position ⑩, the values
also changed in a clockwise half circle from 2 s to 10 min but did
not overlap with the trajectory of the a*b* values for position ⑤.
Figure 8b depicts the relationship between the estimated
effective voltage at positions ⑤ and ⑩ and the corresponding
reaction time. In both positions, the effective voltage rapidly
increased by the first minute of electrolysis and slowly increased
thereafter. In the case of position ⑩, the estimated effective
voltages were 19, 25, 28, 33, and 35 V after the bipolar
anodization for 2, 5, 10, and 30 s and 1 min, respectively. The
effective voltage clearly increased with the increase in the
reaction time. After a 10 min bipolar anodization, the effective
voltage reached 38 V at position ⑩. The thickness of the barrier-
type TiO$_2$ film at position ⑩ was roughly estimated at 70 nm.

The highest value of 38 V was close to the voltage of 43 V (60
$\times \frac{5}{7}$) estimated from eq 1 and corresponded to approximately
63% of the voltage applied to the external driving electrodes.
Thus, the highest anodic potential at the anodic edge of the Ti
BPE estimated from eq 1 was considered to represent ΔV_{BPE}, at
which the redox reaction was saturated. In practice, however, the
effective voltage and the reaction area varied with time,
especially over a short period of time in the early electrolysis
stages. In this study, the oxidized area on the Ti BPE was
visualized using an interference color caused by the formation of
a barrier-type oxide film on the BPE under a DC electric field.
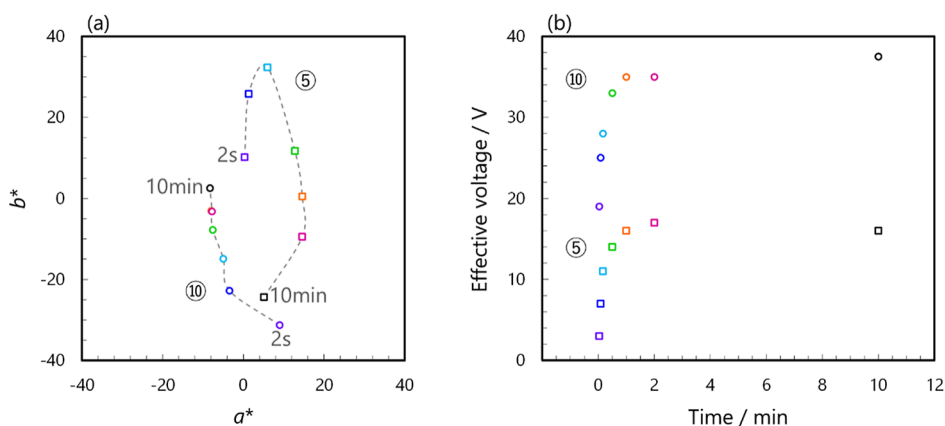The oxidized area of the Ti BPE was coated with Ti oxide, which

Figure 8. (a) a*b* color space and (b) relationship between the estimated effective voltage and DC bipolar anodization times. Data at positions ⑤ and
⑩ on the BPE are shown.

has a wide variety of properties, including catalytic, photo-catalytic, and antibacterial properties. Because the surfaces of the Ti BPEs have structural gradients, the functional surfaces can be used as a sensing and screening device, as previously reported.[3,6] Janus-like electrodes will open new possibilities for multifunctional electrodes.

CONCLUSIONS

In this study, the temporal change in the anodic oxidation area on the Ti BPE horizontally positioned in the cell was visually evaluated by the interference color determined by the thickness of the barrier-type oxide film. The film thickness almost linearly increased from the cathodic site to the edge of the anodic pole of the Ti BPE. Reflecting the asymmetric electric field distribution, the effective voltage was graduated. Note that the anodic oxidation area increased along the longitudinal axis of the BPE with the increasing electrolysis time. For the electrolysis times longer than 10 s, the oxidation area reached 90% of the Ti BPE. The film thickness also rapidly increased by the first minute of the electrolysis and slowly increased thereafter. These findings obtained using spectrophotometry are useful for understanding the phenomena of the BPE, especially during the short period of time in the early electrolysis stages. Further experiments with deeper insights will allow for a more precise reaction control in bipolar electrochemistry.

ASSOCIATED CONTENT

Ⓢ Supporting Information

The Supporting Information is available free of charge at https://pubs.acs.org/doi/10.1021/acsomega.3c01957.

> XRD pattern, surface appearance, *a*b* color space, and *L*a*b* values (PDF)

AUTHOR INFORMATION

Corresponding Author

Hidetaka Asoh — *Department of Applied Chemistry, Kogakuin University, Tokyo 192-0015, Japan;* ⓞ orcid.org/0000-0003-0722-9994; Email: asoh@cc.kogakuin.ac.jp

Author

Yuuka Kokubo — *Department of Applied Chemistry, Kogakuin University, Tokyo 192-0015, Japan*

Complete contact information is available at:
https://pubs.acs.org/10.1021/acsomega.3c01957

Author Contributions

The manuscript was written with contributions from all authors. All authors have given approval to the final version of the manuscript.

Notes

The authors declare no competing financial interest.

ACKNOWLEDGMENTS

ABBREVIATIONS

DC, direct current; BPE, bipolar electrode; Ti, titanium; FESEM, field-emission scanning electron microscopy; XRD, X-ray diffractometry

REFERENCES

(1) Fosdick, S. E.; Knust, K. N.; Scida, K.; Crooks, R. M. Bipolar Electrochemistry. *Angew. Chem., Int. Ed. Engl.* **2013**, *52*, 10438−10456.

(2) Loget, G.; Zigah, D.; Bouffier, L.; Sojic, N.; Kuhn, A. Bipolar Electrochemistry: From Materials Science to Motion and Beyond. *Acc. Chem. Res.* **2013**, *46*, 2513−2523.

(3) Loget, G.; So, S.; Hahn, R.; Schmuki, P. Bipolar Anodization Enables the Fabrication of Controlled Arrays of TiO₂ Nanotube. *J. Mater. Chem. A* **2014**, *2*, 17740−17745.

(4) Wei, W.; Björefors, F.; Nyholm, L. Hybrid Energy Storage Devices Based on Monolithic Electrodes Containing Well-Defined TiO₂ Nanotube Size Gradients. *Electrochim. Acta* **2015**, *176*, 1393−1402.

(5) Koefoed, L.; Pedersen, S. U.; Daasbjerg, K. Bipolar Electrochemistry—A Wireless Approach for Electrode Reactions. *Curr. Opin. Electrochem.* **2017**, *2*, 13−17.

(6) Mu, P.; Li, Y.; Zhang, Y.; Yang, Y.; Hu, R.; Zhao, X.; Huang, A.; Zhang, R.; Liu, X.; Huang, Q.; Lin, C. High-Throughput Screening of Rat Mesenchymal Stem Cell Behavior on Gradient TiO₂ Nanotubes. *ACS Biomater. Sci. Eng.* **2018**, *4*, 2804−2814.

(7) Shida, N.; Zhou, Y.; Inagi, S. Bipolar Electrochemistry: A Powerful Tool for Electrifying Functional Material Synthesis. *Acc. Chem. Res.* **2019**, *52*, 2598−2608.

(8) Sopha, H.; Hromadko, L.; Motola, M.; Macak, J. M. Fabrication of TiO₂ Nanotubes on Ti Spheres using Bipolar Electrochemistry. *Electrochem. Commun.* **2020**, *111*, 106669.

(9) Wu, J.; Li, M.; Zhou, Y.; Geng, W.; Li, X.; Li, K.; Xu, K.; Yang, Y.; Gao, P.; Cai, K. High-Throughput Fabrication of TiO₂ Nanotube Arrays by 4-Electrode Bipolar Electrochemistry. *Scr. Mater.* **2022**, *221*, 114947.

(10) Zhang, Q.; Zhou, H.; Yang, M.; Tang, X.; Hong, Q.; Yang, Z.; Liu, S.; Chen, J.; Zhou, G.; Pan, C. Fabrication and Formation Mechanism of Gradient TiO₂ Nanotubes via Bipolar Anodization. *J. Electroanal. Chem.* **2022**, *915*, 116337.

(11) Asoh, H.; Ishino, M.; Hashimoto, H. Indirect Oxidation of Aluminum Under an AC Electric Field. *RSC Adv.* **2016**, *6*, 90318−90321.

(12) Asoh, H.; Ishino, M.; Hashimoto, H. AC-Bipolar Anodization of Aluminum: Effects of Frequency on Thickness of Porous Alumina Films. *J. Electrochem. Soc.* **2018**, *165*, C295−C301.

(13) Asoh, H.; Miura, S.; Hashimoto, H. One-pot Synthesis of Pt/Alumina Composites via AC-Bipolar Electrochemistry. *ACS Appl. Nano Mater.* **2019**, *2*, 1791−1795.

(14) Asoh, H.; Takeuchi, R.; Hashimoto, H. Unusual Surfaces with Structural Gradients: Investigation of Potential Gradients on Bipolar Electrodes During Bipolar Anodization of Aluminum. *Electrochem. Commun.* **2020**, *120*, 106849.

(15) Asoh, H.; Ishizuka, F.; Kuroki, S.; Takeuchi, R. DC Bipolar Anodization of Aluminum: Wider Anode Area than Expected on the Bipolar Electrodes. *Electrochem. Commun.* **2021**, *125*, 107015.

(16) Takeuchi, R.; Asoh, H. Effects of Size and Position of an Unconnected Aluminum Electrode on Bipolar Anodization in an AC Electric Field. *Sci. Rep.* **2021**, *11*, 22496.

(17) Kokubo, Y.; Asoh, H. Two-step Bipolar Anodization: Design of Titanium with Two Different Faces. *Electrochem. Commun.* **2022**, *142*, 107376.

(18) Asoh, H.; Mizota, K.; Kokubo, Y. Design of Multiphase Metal Balls via Maskless Localized Anodization Based on Bipolar Electrochemistry. *Adv. Mater. Interfaces* **2023**, *10*, 2201835.

(19) Sul, Y. T.; Johansson, C. B.; Jeong, Y.; Albrektsson, T. The Electrochemical Oxide Growth Behaviour on Titanium in Acid and Alkaline Electrolytes. *Med. Eng. Phys.* **2001**, *23*, 329−346.

(20) Van Gils, S. V.; Mast, P.; Stijns, E.; Terryn, H. Colour Properties of Barrier Anodic Oxide Films on Aluminium and Titanium Studied with Total Reflectance and Spectroscopic Ellipsometry. *Surf. Coat. Technol.* **2004**, *185*, 303−310.

(21) Diamanti, M. V.; Del Curto, B.; Pedeferri, M. Interference Colors of Thin Oxide Layers on Titanium. *Color Res. Appl.* **2008**, *33*, 221−228.